

# Methane-carbon budget of a ferruginous meromictic lake and implications for marine methane dynamics on early Earth

Sajjad A. Akam<sup>1,\*</sup>, Pei-Chuan Chuang<sup>2,3,\*</sup>, Sergei Katsev<sup>4</sup>, Chad Wittkop<sup>5</sup>, Michelle Chamberlain<sup>3</sup>, Andrew W. Dale<sup>2</sup>, Klaus Wallmann<sup>2</sup>, Adam J. Heathcote<sup>6</sup>, and Elizabeth D. Swanner<sup>1</sup>

<sup>1</sup>Department of Geological and Atmospheric Sciences, Iowa State University, Ames, Iowa 50011, USA

<sup>2</sup>GEOMAR, Helmholtz Centre for Ocean Research, 24148 Kiel, Germany

<sup>3</sup>Department of Earth Sciences, National Central University, Taoyuan City, Taiwan 320

<sup>4</sup>Department of Physics, University of Minnesota–Duluth, Duluth, Minnesota 55812, USA

<sup>5</sup>Department of Biochemistry, Chemistry, and Geology, Minnesota State University, Mankato, Minnesota 56001, USA

<sup>6</sup>St. Croix Watershed Research Station, Science Museum of Minnesota, Marine on St. Croix, Minnesota 55047, USA

## ABSTRACT

The greenhouse gas methane (CH<sub>4</sub>) contributed to a warm climate that maintained liquid water and sustained Earth's habitability in the Precambrian despite the faint young sun. The viability of methanogenesis (ME) in ferruginous environments, however, is debated, as iron reduction can potentially outcompete ME as a pathway of organic carbon remineralization (OCR). Here, we document that ME is a dominant OCR process in Brownie Lake, Minnesota (midwestern United States), which is a ferruginous (iron-rich, sulfate-poor) and meromictic (stratified with permanent anoxic bottom waters) system. We report ME accounting for  $\geq 90\%$  and  $>9\% \pm 7\%$  of the anaerobic OCR in the water column and sediments, respectively, and an overall particulate organic carbon loading to CH<sub>4</sub> conversion efficiency of  $\geq 18\% \pm 7\%$  in the anoxic zone of Brownie Lake. Our results, along with previous reports from ferruginous systems, suggest that even under low primary productivity in Precambrian oceans, the efficient conversion of organic carbon would have enabled marine CH<sub>4</sub> to play a major role in early Earth's biogeochemical evolution.

## INTRODUCTION

The greenhouse gas methane (CH<sub>4</sub>), with a present atmospheric concentration of 1.8 ppmv, contributes  $\leq 25\%$  of postindustrial global warming (Etminan et al., 2016). The importance of CH<sub>4</sub> to Precambrian climate may have been considerably higher, with estimated atmospheric concentrations ranging from 600 to 3000 ppmv in the Archean and 1 to 100 ppmv in the Proterozoic (Fig. 1; Olson et al., 2016; Fakrae et al., 2019). Methane concentrations may have played multiple roles in early Earth's biogeochemical evolution, among others: in contributing to greenhouse gas warming under a faint young sun to maintain warm surface temperature, liquid water, and Earth's habitability (Haqq-Misra et al., 2008); in producing an anti-greenhouse organic haze layer (Pavlov et al., 2001); in drawing down the H<sub>2</sub>-based greenhouse warming, leading to a late Archean (2.9 Ga) glaciation event (Wordsworth


and Pierrehumbert, 2013); in contributing to hydrogen escape to space, leading to oxidation of Earth's surface environment (Catling et al., 2001); in decreasing microbial methanogenesis (ME), leading to oxygen buildup in the atmosphere (Konhauser et al., 2009); and in decreasing atmospheric CH<sub>4</sub> levels, contributing to the onset of Proterozoic glaciations (Zahnle et al., 2006). All these hypotheses require an active CH<sub>4</sub> cycle, likely with biological mediation. ME is one of the oldest microbial metabolic pathways. Its origin is dated back to  $>3.5$  Ga, and it is considered to have played an essential role in CH<sub>4</sub> supply to the atmosphere during Earth's early history (Kharecha et al., 2005). Ferruginous conditions were a dominant feature of Earth's early oceans (Fig. 1; Poulton, 2021), and so an understanding of the role of ME under ferruginous conditions is essential to our understanding of marine carbon cycling in early Earth.

Meromictic ferruginous lakes are considered to be convenient analogs to Precambrian oceans (Swanner et al., 2020). Such lakes generally have large reservoirs of CH<sub>4</sub> (1–4 mM in bottom

waters; Crowe et al., 2011; Lopes et al., 2011). However, estimates of the amount of organic carbon (OC) that is degraded by ME have only been calculated for a handful of lakes, with estimated particulate organic carbon to CH<sub>4</sub> remineralization efficiency varying even within a single lake, i.e., Lake Matano, from 3% to 80% (Crowe et al., 2011; Kuntz et al., 2015). Ferruginous conditions, or rather the scarcity of sulfate, likely promote ME as the dominant pathway of organic carbon remineralization (OCR) (Friese et al., 2021). Yet, some researchers have proposed that ME plays only a minor role in ferruginous oceans (Laakso and Schrag, 2019). The efficiency of ME during OCR in ancient ferruginous oceans is thus poorly constrained. Here, we report the carbon budget for OCR and ME in Brownie Lake, a ferruginous meromictic lake that is biogeochemically analogous to Precambrian oceans (Lambrecht et al., 2018), and we evaluate the implications for Precambrian CH<sub>4</sub>-carbon dynamics. Our results highlight that ME is a dominant OCR pathway in sulfate-poor ferruginous aquatic systems, suggestive of large CH<sub>4</sub> storage in and fluxes from/to the Precambrian ferruginous oceans, thereby supporting models that invoke the importance of CH<sub>4</sub> in Earth's early climate.

## STUDY SITE

Brownie Lake (44°58'04"N, 93°19'26"W) is the northernmost lake in the Minneapolis Chain of Lakes, Minnesota, upper midwestern United States (Fig. 2), and it was characterized in detail by Lambrecht et al. (2018). It is a eutrophic lake with abundant iron in the anoxic water column and sediments. This lake has been meromictic since 1925, and its long-term water-column stratification results in strong physicochemical

Sajjad A. Akam  <https://orcid.org/0000-0002-6089-0370>  
\*sajjad@iastate.edu; peichuanchuang@ncu.edu.tw

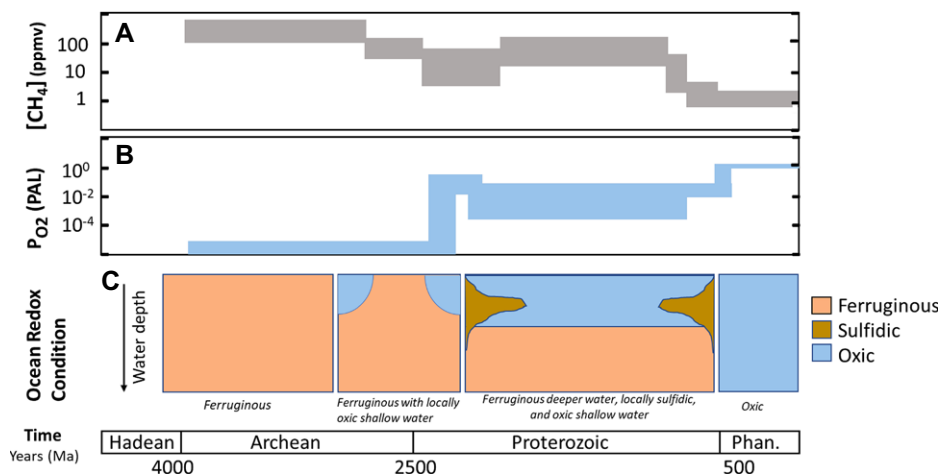


**Figure 1. (A) Atmospheric CH<sub>4</sub> concentration and (B) atmospheric O<sub>2</sub> concentration (Fakhræe et al., 2019). (C) Spatially predominant ocean-redox conditions over Earth's history (Poulton, 2021). PAL—present atmospheric level.**

gradients of sunlight, oxygen, and iron (Lambrech et al., 2018). Brownie Lake currently has a maximum depth of 14 m and a surface area of 5 ha. The conductivity, dissolved O<sub>2</sub>, and temperature profiles indicate an oxic mixolimnion (0–3.5 m) and a dense anoxic monimolimnion below 5 m, separated by a chemocline (4–5 m), which often coincides with the oxycline (Fig. 2). Previous 16S ribosomal ribonucleic acid (rRNA) sequencing revealed that methanogens, primarily of the order Methanobacteriales, are abundant in the water column (Lambrech et al., 2020). At 11–12 m water depth, methanogen sequences accounted for ~31% of sequences, with a biogenic δ<sup>13</sup>C<sub>CH<sub>4</sub></sub> signature (−64‰) and a higher CH<sub>4</sub> concentration compared to the nearest sediment—pointing to active water-column methanogenesis (Lambrech et al., 2020). Aerobic methanotrophy is the dominant CH<sub>4</sub> oxidation mechanism (Lambrech et al., 2020). We built on these previous results from this lake by incorporating OC fluxes, sediment burial rates, and OCR rates, along with a reaction transport model, to evaluate the role of ME in OC cycling.

## METHODS

Water-column profiles of concentrations and stable carbon isotopes of CH<sub>4</sub> (δ<sup>13</sup>C<sub>CH<sub>4</sub></sub>), dissolved and particulate organic carbon (δ<sup>13</sup>C<sub>DOC</sub>, δ<sup>13</sup>C<sub>POC</sub>), and dissolved inorganic carbon (δ<sup>13</sup>C<sub>DIC</sub>), along with concentrations of major nutrients, anions, and cations in Brownie Lake, were collected over several years (Swanner et al., 2022). This study utilized previously reported CH<sub>4</sub>, dissolved inorganic carbon (DIC), and major nutrient, anion, and cation data (Lambrech et al., 2018, 2020) along with new data, including concentrations of particulate organic carbon (POC), dissolved organic carbon (DOC), particulate organic nitrogen (PON), and dissolved organic nitrogen (DON), along with their isotopic compositions, to quantify the lake's OC budget. Primary productivity and external carbon loading were quantified

using rapid light curves and the external chemical input model available for Brownie Lake (Section 2 in the Supplemental Material<sup>1</sup>). A 1.5-m-long sediment piston core was collected from the deep basin for <sup>210</sup>Pb dating using the constant rate of supply model to quantify dry mass accumulation rates (Appleby and Oldfield, 1978; Supplemental Material Section 3). To investigate and quantify the processes controlling the distribution of dissolved and particulate species as well as the turnover of C, S, Fe, and P in the water column, the data from the lake were simulated with an existing biogeochemical reaction transport model (Dale et al., 2009; Supplemental Material Section 4). The August 2018 data set was the most comprehensive for the above chemical species and was used for reaction transport modeling. OCR in the sediment column was constrained by mass-balancing the measured sediment OC burial and modeled OC rain rate to the lake floor.

## RESULTS AND DISCUSSION

The POC loading was 107–264 mmol C m<sup>-2</sup> d<sup>-1</sup> with contributions from primary productivity (100–250 mmol C m<sup>-2</sup> d<sup>-1</sup>) and runoff (7–14 mmol C m<sup>-2</sup> d<sup>-1</sup>; Supplemental Material Section 2). Water-column profiles showed a subsurface chlorophyll maximum at 3.5 m, characteristic of ferruginous meromictic lakes, along with a positive spike in POC, PON, and DOC, and a low C:N ratio (total organic carbon[TOC]/total nitrogen [TN] mass/mass) (Fig. 3; Supple-

<sup>1</sup>Supplemental Material. Additional information on lake setting, water chemistry measurements, organic carbon loading calculation, sediment coring, age dating, mass accumulation rates, reaction transport model description, δ<sup>13</sup>C and C:N compositions for organic carbon source identification, oxidation state of iron in sediments, methane storage comparison with lakes of similar size, and overall carbon cycling schematic. Please visit <https://doi.org/10.1130/GEOL.S.24891486> to access the supplemental material; contact [editing@geosociety.org](mailto:editing@geosociety.org) with any questions.

mental Material Section 1), indicating a predominantly autochthonous labile OC flux sinking to the deeper water column. The increases in ammonium and DIC concentrations with depth in the monimolimnion (below 4–5 m) indicate OCR. Increasing δ<sup>13</sup>C<sub>DIC</sub> values (−11.53‰ at 3.5 m to −2.92‰ at 13 m depth) and CH<sub>4</sub> concentrations (maximum of 0.2 mM above 3.5 m to maximum of 1.5 mM in the monimolimnion) with depth indicate active ME below the chemocline. The DOC concentration profile below the chemocline did not show comparable variation with DIC and CH<sub>4</sub> concentrations, indicating that only a portion of the OC is available for ME, and there is a sizeable recalcitrant DOC pool. Depletion of <sup>13</sup>C<sub>DIC</sub>, <sup>13</sup>C<sub>DOC</sub>, and <sup>13</sup>C<sub>POC</sub>, along with enrichment in <sup>13</sup>C<sub>CH<sub>4</sub></sub> at the chemocline, suggests strong aerobic CH<sub>4</sub> oxidation above the chemocline (Fig. 2; cf. Lambrecht et al., 2020). CH<sub>4</sub> storage was estimated by integrating measured CH<sub>4</sub> concentration to water volume data per depth and lake surface area, yielding 25.85 g C m<sup>-2</sup>, which is very high compared to other lakes with similar surface areas (Supplemental Material Section 7).

Our reaction transport model-based simulation for POC remineralization in the water column returned a good fit to the measured chemical parameters (Fig. 3; Supplemental Material Section 4). Results yielded a total OCR rate of 67–224 mmol C m<sup>-2</sup> d<sup>-1</sup> (62%–85% of POC loading), of which 28–37 mmol C m<sup>-2</sup> d<sup>-1</sup> (14%–26% of POC loading) occurred in the water column (Table 1). Here, 75% ± 1% of water-column OCR occurred anaerobically, of which ME accounted for 92%–95% (19–27 mmol C m<sup>-2</sup> d<sup>-1</sup>; Table 1). The OCR via sulfate reduction and dissimilatory iron reduction in the water column was limited in comparison (1.6 ± 0.1 mmol C m<sup>-2</sup> d<sup>-1</sup>; 5%–8% of anaerobic OCR). The excess ammonium observed below the redoxcline compared to the modeled result could be due to nitrogen fixation (Philippi et al., 2021) or dissimilatory nitrate reduction to ammonium instead of N<sub>2</sub> (Michiels et al., 2017), two processes that have been observed in ferruginous lakes. While iron reduction could be thermodynamically favorable in the Brownie Lake water column, our results suggest a minimal role for dissimilatory iron reduction in OCR. Previous studies have shown that methanogens can outcompete iron reducers during OCR in non-carbon-limited settings due to the transformation of iron-oxide minerals to stable forms or due to surface passivation of reactive iron oxides by Fe(II) (Friese et al., 2021; Gadol et al., 2022). The presence of iron-oxide minerals in the sediments (Supplemental Material Section 6) indicates they are escaping water-column remineralization processes, thereby favoring ME as the dominant mode of OCR in the monimolimnion.

The modeled OC rain rate at the lake floor (79–226 mmol C m<sup>-2</sup> d<sup>-1</sup>; 74%–86% of total OC load) combined with the measured OC

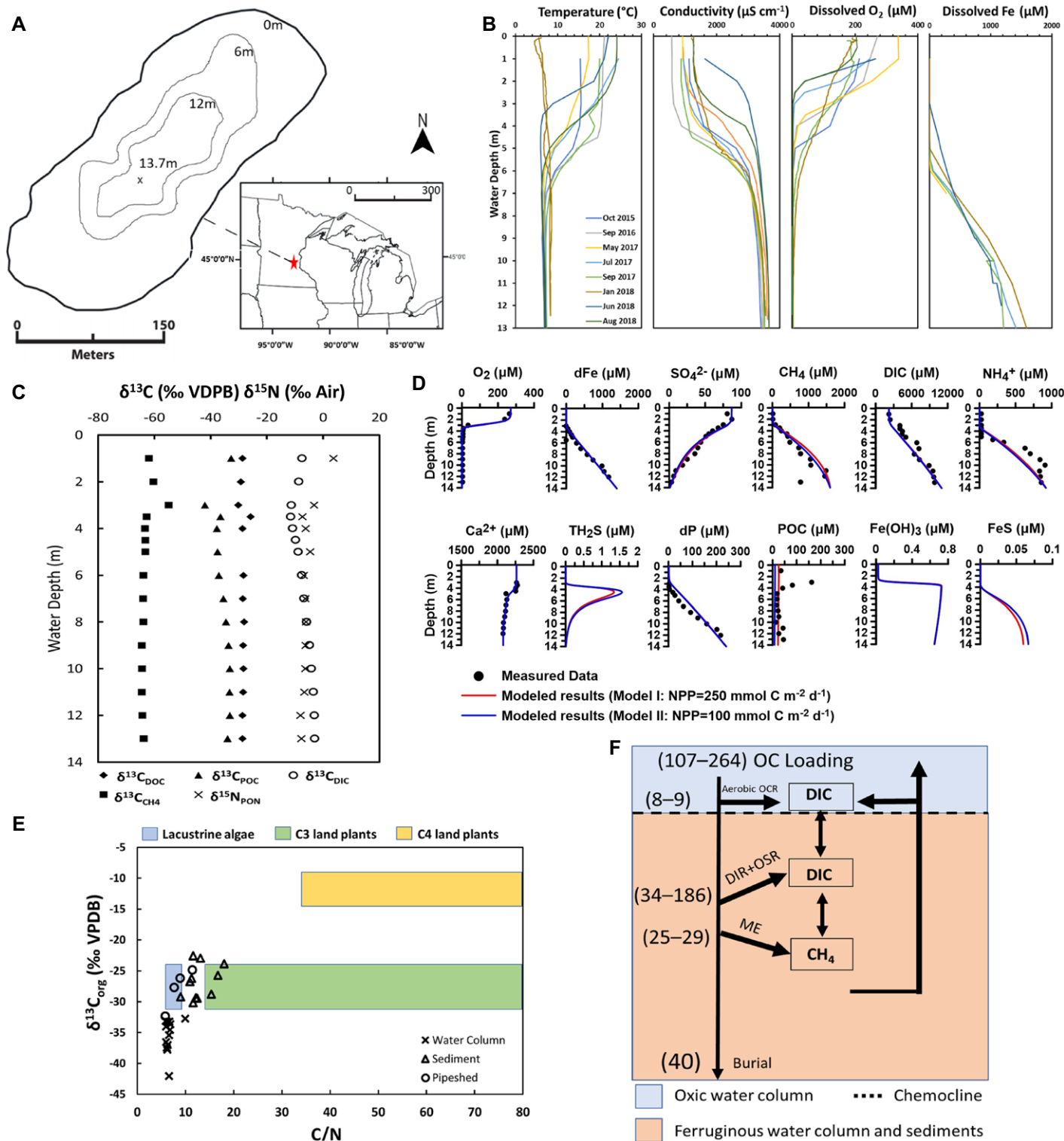


**Figure 2.** (A) Study site. (B) Temperature, conductivity, and dissolved  $\text{O}_2$  and Fe profiles of water column. (C) Isotopic compositions of water column. (D) Measured and modeled water-column concentration profiles. DIC—dissolved inorganic carbon; POC—particulate organic carbon; NPP—net primary productivity. (E) Cross-plot of total organic carbon (TOC):N and  $\delta^{13}\text{C}_{\text{org}}$  suggestive of labile carbon availability (Meyers, 1994). VPDB—Vienna Pee Dee belemnite. (F) Overall carbon budget schematic. OC—organic carbon; OCR—organic carbon remineralization; ME—methanogenesis; DIR + OSR—dissimilatory iron reduction and organoclastic sulfate reduction. Pipesheds are channels of external drainage input.

burial ( $40.38 \text{ mmol C m}^{-2} \text{ d}^{-1}$  for top 11 cm and  $37.78 \text{ mmol C m}^{-2} \text{ d}^{-1}$  for top 70 cm) point to  $38\text{--}186 \text{ mmol C m}^{-2} \text{ d}^{-1}$  OCR in the sediment column and that only 18%–51% of the OC rain is

being buried. This OCR in the ferruginous sediment column would occur via dissimilatory iron reduction and ME (Bray et al., 2017). The modeled  $\text{CH}_4$  flux from the sediment column toward

the lake floor ( $1\text{--}3 \text{ mmol CH}_4 \text{ m}^{-2} \text{ d}^{-1}$ ) implies a minimum methanogenic OCR of  $2\text{--}6 \text{ mmol C m}^{-2} \text{ d}^{-1}$  in the sediment column. We emphasize that this is the minimum ME estimate in the

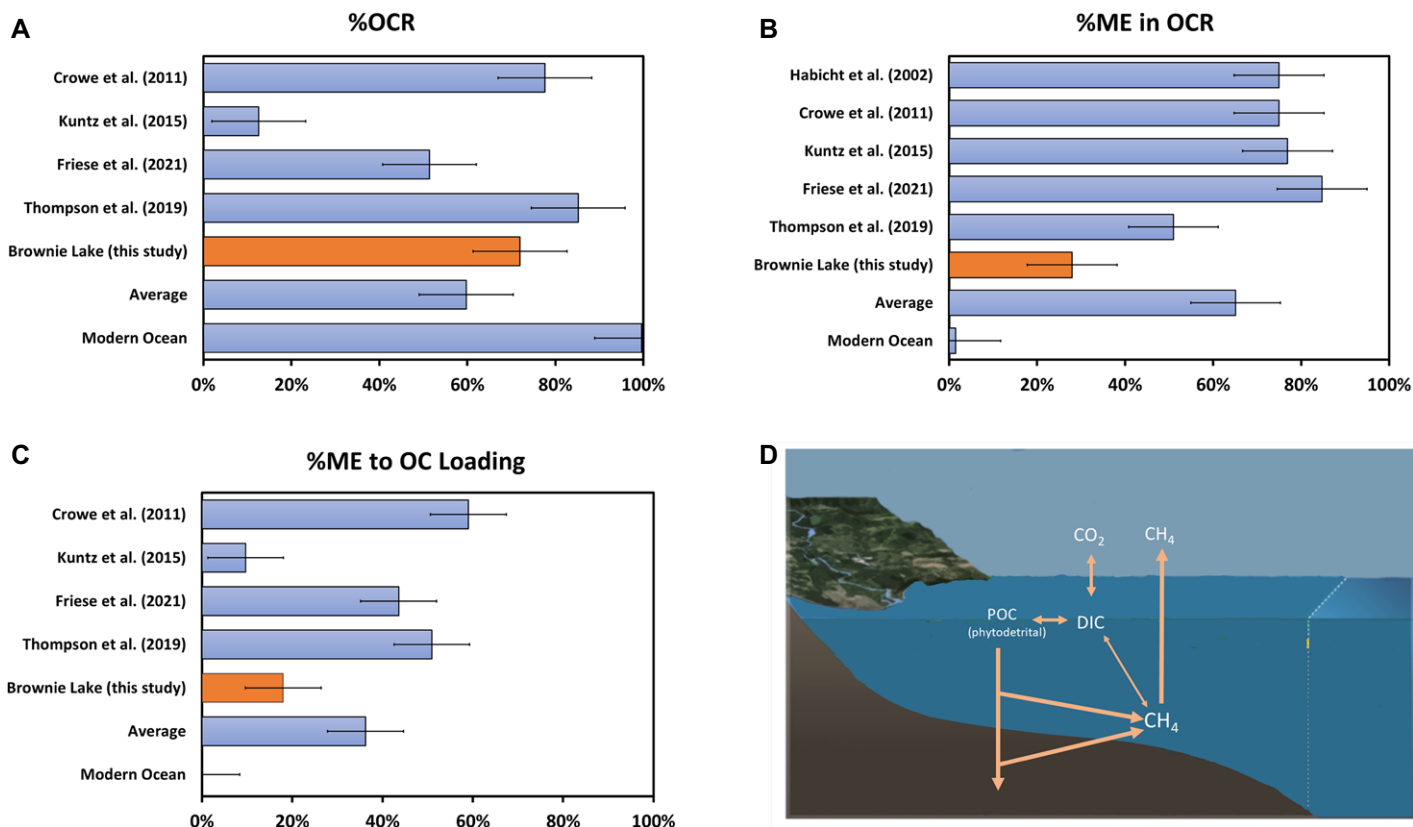


**Figure 3.** Comparison of (A) anaerobic organic carbon remineralization (OCR) rates for Archean ferruginous settings and analogs, (B) efficiency of methanogenesis (ME) in OCR, and (C) ME efficiency to organic carbon (OC) loading (data from Table S7 [see text footnote 1]). (D) Simplified schematic of C-CH<sub>4</sub> cycling in ancient ferruginous oceans. DIC—dissolved inorganic carbon; POC—particulate organic carbon.

sediment, since a portion of CH<sub>4</sub> produced in the sediment column could be consumed by Fe-dependent anaerobic oxidation of ethane (Crowe et al., 2011; Supplemental Material Section 6). The low C:N ratio and low  $\delta^{13}\text{C}_{\text{org}}$  values in the benthic nepheloid layer and sediment column, along with highly enriched  $\delta^{13}\text{C}_{\text{DIC}}$  values for the top 40 cm of measured pore water (Fig. S5), support the interpretation of active ME in shallow sediments. Taken together, ME accounted for at least 13%–42% of anaerobic OCR in the ferruginous water column and sediments.

Evaluation of the role of ME in ancient ferruginous oceans will provide critical insights into the carbon cycling dynamics during the Precambrian and Earth's early climate evolution. Comparison of Brownie Lake's CH<sub>4</sub>-carbon budget with other published data sets (Fig. 3) suggests that the reported OC loading to CH<sub>4</sub> conversion efficiency in anaerobic OCR under ferruginous settings averages 36% (18%–59%), with Brownie Lake at the lower end of this range but still significantly higher than modern (oxic) oceans, which have 0.1% efficiency. OC burial

and ME could have impacted Earth's early oxygenation in different ways—the former removes a reductant from Earth's surface, and the latter injects a reductant into the atmosphere, inducing greenhouse warming and contributing to top-down oxygenation via hydrogen escape to space (after CH<sub>4</sub> photolysis) from the atmosphere (Catling et al., 2001). A dominant role for CH<sub>4</sub> in the Precambrian climate has been widely proposed in the past three decades of literature (Catling and Zahnle, 2020). A few recent studies have argued for a limited role for

TABLE 1. SUMMARY OF MODELED CARBON CYCLING PARAMETERS IN BROWNIE LAKE, MINNESOTA, USA

Water column		Sediment column		Sediment and water column	
OC load	107–264	OC rain to sediment	78.820–226.49	OC load	107–264
OCR via O <sub>2</sub>	7.33–11.78	ME	1.95–5.98	Total OCR	66.60–223.5
OCR via SR	1.52–1.71	OC burial	40.38	ME	25.08–28.69
OCR via IR	0.03–0.04	Total OCR in sediment	38.44–186.11	Total OCR via non-ME	41.53–194.81
ME	19.10–26.74	Non-ME OCR in sediment	32.46–184.16	OC burial	40.38
Total OCR in water column	28.16–37.39	% OCR in sediment to OC rain	49–82	% non-ME OCR to OC load	62–87
OC rain to sediment	79–226	% ME of sediment OC load	1–8	% ME to total OC load	11–23
% anaerobic OCR in water column	74–76	% anaerobic OCR in sediment column	100	% ME to total anaerobic OCR	13–42
% OCR in water column to OC load	14–26	% ME of sediment OCR (min)*	1–16	% ME to total OCR	13–38
% ME to OC load	10–18	% non-ME degradation to sediment OCR	84–99	% burial to total OC load	15–38
% ME of water-column OCR	67–72	% OC rain to sediment to OC load in water column	74–86	% total OCR to total OC load	62–85
% OCR in water column via O <sub>2</sub>	24–26	% burial of OC rain to sediment	18–51	% OC load degraded via non-ME processes	39–74
% OC load to sediment rain	74–86	% burial to OC load at water surface	15–38	% ME to OC loading below the chemocline	11–25

Notes: All units besides percentages are in mmol C m<sup>-2</sup> d<sup>-1</sup>. OC—organic carbon; OCR—organic carbon remineralization; SR—sulfate reduction; IR—iron reduction; ME—methanogenesis. OCR and ME in sediment column were derived based on water-column OCR, OC rain to sediment column, and measured whole lake sediment burial rates. This is the lower limit of ME if there is CH<sub>4</sub> and OC oxidation in sediments. If there is deeper flux, it could lower the ME rate. Our value is a balanced approximation considering both factors. Refer to Supplemental Material Section 4 for detailed model results (see text footnote 1).

\*ME in sediments is the minimum value if anaerobic methane oxidation occurs in sediment column.

CH<sub>4</sub> in the Precambrian climate (Laakso and Schrag, 2019), citing a case example of high OC burial in ferruginous Lake Matano (Kuntz et al., 2015). Our results from Brownie Lake rather support a lower proportion of OC being buried in sediments under ferruginous settings and a dominant role for CH<sub>4</sub> in the Archean carbon cycle (Thompson et al., 2019).

In the modern oceans, an average net primary productivity (NPP) of 50 Gt C yr<sup>-1</sup> results in 2 Gt C yr<sup>-1</sup> deposited in the seafloor, leading to ~0.05 Gt CH<sub>4</sub> yr<sup>-1</sup> ME via OCR (Akam et al., 2023), with an OC loading to CH<sub>4</sub> generation efficiency of 0.1%. Estimates for a late Archean setting range from 0.1% to 14% of modern NPP (Ward et al., 2019; Farr et al., 2023). An OC to CH<sub>4</sub> conversion efficiency of 36% would yield 2–210 (extended range of 1–344 considering 18%–59% efficiency) Tmol CH<sub>4</sub> yr<sup>-1</sup> or 0.4–56 times modern annual marine ME rates (Supplemental Material Section 8). Interestingly, Ozaki et al. (2018) modeled an increased efficiency of CH<sub>4</sub> cycling under a hybrid ecosystem composed of H<sub>2</sub> and Fe<sup>2+</sup>-based anoxygenic photoautotrophy. Under low-sulfate and low-oxygen surface waters, this CH<sub>4</sub> would have entered the atmosphere easily, compared to >90% CH<sub>4</sub> being oxidized in the modern ocean with high sulfate and oxygen (Habicht et al., 2002).

Photochemical models predict that the lifetime of CH<sub>4</sub> in a low-O<sub>2</sub> atmosphere is 5000–10,000 yr, as opposed to ~12 yr today (Catling et al., 2001). Hence, the anoxic Archean atmosphere could have held thousands of parts per million by volume of CH<sub>4</sub>, provided a sufficient CH<sub>4</sub> supply, and even a smaller CH<sub>4</sub> flux over time (e.g., 2 Tmol CH<sub>4</sub> yr<sup>-1</sup> in the Archean over thousands of years) could have increased CH<sub>4</sub>-induced warming on early Earth. The gradual oxidation of Earth's surface would have limited ME to anoxic deep water and the sediment column as well as reduced the lifetime of CH<sub>4</sub> in the atmosphere, limiting their warming control mechanisms (Olson et al., 2016). Our results point to efficient ME in ancient ferruginous oceans, supporting the climate models and suggesting significant climate warming by CH<sub>4</sub> (Haqq-Misra et al., 2008). In contrast, a lesser role from CH<sub>4</sub> warming was proposed recently, primarily based on high OC burial rates in Lake Matano (Laakso and Schrag, 2019). Our results hence emphasize that the ferruginous oceans were conducive to high rates of ME, and thus the availability of OC loading and oxidants like sulfate and oxygen would have been the key controlling factors determining the marine CH<sub>4</sub> fluxes to Earth's early atmosphere. The amount of CH<sub>4</sub> produced would have closely followed the trend of NPP in early Earth until the advent of surface oxygenation, at which time the efficiency of ME with reference to NPP would have decreased gradually, leading to the current efficiency of 0.1%. Last, we highlight the need to constrain the OC budget and the

relative efficiency of ME from additional ferruginous systems to improve our understanding of the biogeochemical significance of iron-rich systems at present and in the geological past.

## CONCLUSION

We documented that ME is a dominant OCR process in ferruginous meromictic Brownie Lake, accounting for ≥90% and >9% ± 7% of the anaerobic OCR in the water column and sediments, respectively, and we calculated an overall POC loading to CH<sub>4</sub> conversion efficiency of ≥18% ± 7% in the anoxic zone of Brownie Lake. Our results, combined with available results from other ferruginous systems, point to a very high conversion efficiency (36% ± 21%) of POC to CH<sub>4</sub> in these systems, compared to 0.1% in the modern sulfatic and oxic ocean. Hence, we conclude that even under a low primary productivity scenario, Archean oceans would have produced sufficient CH<sub>4</sub> to have influenced early Earth's biogeochemical evolution, in agreement with climate models suggesting CH<sub>4</sub>-induced greenhouse warming in early Earth.

## ACKNOWLEDGMENTS

National Science Foundation award no. 1944946 to E.D. Swanner and field permits from the Minneapolis Park and Recreation Board are duly acknowledged. We thank Eva Stüeken and two anonymous reviewers for their constructive feedback.

## REFERENCES CITED

- Akam, S.A., Swanner, E.D., Yao, H., Hong, W.-L., and Peckmann, J., 2023, Methane-derived authigenic carbonates—A case for a globally relevant marine carbonate factory: *Earth-Science Reviews*, v. 243, <https://doi.org/10.1016/j.earscirev.2023.104487>.
- Appleby, P.G., and Oldfield, F., 1978, The calculation of lead-210 dates assuming a constant rate of supply of unsupported <sup>210</sup>Pb to the sediment: *Catena*, v. 5, p. 1–8, [https://doi.org/10.1016/S0341-8162\(78\)80002-2](https://doi.org/10.1016/S0341-8162(78)80002-2).
- Bray, M.S., Wu, J., Reed, B.C., Kretz, C.B., Belli, K.M., Simister, R.L., Henny, C., Stewart, F.J., DiChristina, T.J., Brandes, J.A., Fowle, D.A., Crowe, S.A., and Glass, J.B., 2017, Shifting microbial communities sustain multiyear iron reduction and methanogenesis in ferruginous sediment incubations: *Geobiology*, v. 15, p. 678–689, <https://doi.org/10.1111/gbi.12239>.
- Catling, D.C., and Zahnle, K.J., 2020, The Archean atmosphere: *Science Advances*, v. 6, <https://doi.org/10.1126/sciadv.aax1420>.
- Catling, D.C., Zahnle, K.J., and McKay, C.P., 2001, Biogenic methane, hydrogen escape, and the irreversible oxidation of early Earth: *Science*, v. 293, p. 839–843, <https://doi.org/10.1126/science.1061976>.
- Crowe, S.A., et al., 2011, The methane cycle in ferruginous Lake Matano: *Geobiology*, v. 9, p. 61–78, <https://doi.org/10.1111/j.1472-4669.2010.00257.x>.
- Dale, A.W., Brüchert, V., Alperin, M., and Regnier, P., 2009, An integrated sulfur isotope model for Namibian shelf sediments: *Geochimica et Cosmochimica Acta*, v. 73, p. 1924–1944, <https://doi.org/10.1016/j.gca.2008.12.015>.
- Etminan, M., Myhre, G., Highwood, E.J., and Shine, K.P., 2016, Radiative forcing of carbon dioxide, methane, and nitrous oxide: A significant revision

of the methane radiative forcing: *Geophysical Research Letters*, v. 43, p. 12,614–12,623, <https://doi.org/10.1002/2016GL071930>.

- Fakraee, M., Hancisse, O., Canfield, D.E., Crowe, S.A., and Katsev, S., 2019, Proterozoic seawater sulfate scarcity and the evolution of ocean-atmosphere chemistry: *Nature Geoscience*, v. 12, p. 375–380, <https://doi.org/10.1038/s41561-019-0351-5>.
- Farr, O., Hao, J., Liu, W., Fehon, N., Reinfeldt, J.R., Yee, N., and Falkowski, P.G., 2023, Archean phosphorus recycling facilitated by ultraviolet radiation: Proceedings of the National Academy of Sciences of the United States of America, v. 120, <https://doi.org/10.1073/pnas.2307524120>.
- Friese, A., et al., 2021, Organic matter mineralization in modern and ancient ferruginous sediments: *Nature Communications*, v. 12, <https://doi.org/10.1038/s41467-021-22453-0>.
- Gadol, H.J., Elsherbini, J., and Kocar, B.D., 2022, Methanogen productivity and microbial community composition varies with iron oxide mineralogy: *Frontiers in Microbiology*, v. 12, <https://doi.org/10.3389/fmicb.2021.705501>.
- Habicht, K.S., Gade, M., Thamdrup, B., Berg, P., and Canfield, D.E., 2002, Calibration of sulfate levels in the Archean ocean: *Science*, v. 298, p. 2372–2374, <https://doi.org/10.1126/science.1078265>.
- Haqq-Misra, J.D., Domagal-Goldman, S.D., Kasting, P.J., and Kasting, J.F., 2008, A revised, hazy methane greenhouse for the Archean Earth: *Astrobiology*, v. 8, p. 1127–1137, <https://doi.org/10.1089/ast.2007.0197>.
- Kharchea, P., Kasting, J., and Siefert, J., 2005, A coupled atmosphere-ecosystem model of the early Archean Earth: *Geobiology*, v. 3, p. 53–76, <https://doi.org/10.1111/j.1472-4669.2005.00049.x>.
- Konhauser, K.O., Pecoits, E., Lalonde, S.V., Papi-neau, D., Nisbet, E.G., Barley, M.E., Arndt, N.T., Zahnle, K., and Kamber, B.S., 2009, Oceanic nickel depletion and a methanogen famine before the Great Oxidation Event: *Nature*, v. 458, p. 750–753, <https://doi.org/10.1038/nature07858>.
- Kuntz, L.B., Laakso, T.A., Schrag, D.P., and Crowe, S.A., 2015, Modeling the carbon cycle in Lake Matano: *Geobiology*, v. 13, p. 454–461, <https://doi.org/10.1111/gbi.12141>.
- Laakso, T.A., and Schrag, D.P., 2019, Methane in the Precambrian atmosphere: *Earth and Planetary Science Letters*, v. 522, p. 48–54, <https://doi.org/10.1016/j.epsl.2019.06.022>.
- Lambrech, N., Wittkop, C., Katsev, S., Fakraee, M., and Swanner, E.D., 2018, Geochemical characterization of two ferruginous meromictic lakes in the Upper Midwest, USA: *Journal of Geophysical Research: Biogeosciences*, v. 123, p. 3403–3422, <https://doi.org/10.1029/2018JG004587>.
- Lambrech, N., Katsev, S., Wittkop, C., Hall, S.J., Sheik, C.S., Picard, A., Fakraee, M., and Swanner, E.D., 2020, Biogeochemical and physical controls on methane fluxes from two ferruginous meromictic lakes: *Geobiology*, v. 18, p. 54–69, <https://doi.org/10.1111/gbi.12365>.
- Lopes, F., Viollier, E., Thiam, A., Michard, G., Abril, G., Groleau, A., Prévot, F., Carrias, J.F., Albéric, P., and Jézéquel, D., 2011, Biogeochemical modelling of an anaerobic vs. aerobic methane oxidation in a meromictic crater lake (Lake Pavin, France): *Applied Geochemistry*, v. 26, p. 1919–1932, <https://doi.org/10.1016/j.apgeochem.2011.06.021>.
- Meyers, P.A., 1994, Preservation of elemental and isotopic source identification of sedimentary organic matter: *Chemical Geology*, v. 114, p. 289–302, [https://doi.org/10.1016/0009-2541\(94\)90059-0](https://doi.org/10.1016/0009-2541(94)90059-0).
- Michiels, C.C., Darchambeau, F., Roland, F.A.E., Morana, C., Llirós, M., García-Armisen, T., Thamdrup, B., Borges, A.V., Canfield, D.E., Servais, P., Descy, J.-P., and Crowe, S.A., 2017,

- Iron-dependent nitrogen cycling in a ferruginous lake and the nutrient status of Proterozoic oceans: *Nature Geoscience*, v. 10, p. 217–221, <https://doi.org/10.1038/ngeo2886>.
- Olson, S.L., Reinhard, C.T., and Lyons, T.W., 2016, Limited role for methane in the mid-Proterozoic greenhouse: *Proceedings of the National Academy of Sciences of the United States of America*, v. 113, p. 11,447–11,452, <https://doi.org/10.1073/pnas.1608549113>.
- Ozaki, K., Tajika, E., Hong, P.K., Nakagawa, Y., and Reinhard, C.T., 2018, Effects of primitive photosynthesis on Earth's early climate system: *Nature Geoscience*, v. 11, p. 55–59, <https://doi.org/10.1038/s41561-017-0031-2>.
- Pavlov, A.A., Kasting, J.F., Eigenbrode, J.L., and Freeman, K.H., 2001, Organic haze in Earth's early atmosphere: Source of low-<sup>13</sup>C late Archean kerogens?: *Geology*, v. 29, p. 1003–1006, [https://doi.org/10.1130/0091-7613\(2001\)029<1003:OHI ESE>2.0.CO;2](https://doi.org/10.1130/0091-7613(2001)029<1003:OHI ESE>2.0.CO;2).
- Philippi, M., Kitzinger, K., Berg, J.S., Tschitschko, B., Kidane, A.T., Littmann, S., Marchant, H.K., Storelli, N., Winkel, L.H.E., Schubert, C.J., Mohr, W., and Kuypers, M.M.M., 2021, Purple sulfur bacteria fix N<sub>2</sub> via molybdenum-nitrogenase in a low molybdenum Proterozoic ocean analogue: *Nature Communications*, v. 12, 4774, <https://doi.org/10.1038/s41467-021-25000-z>.
- Poulton, S.W., 2021, *The Iron Speciation Paleoredox Proxy*: Cambridge, UK, Cambridge University Press, 34 p., <https://doi.org/10.1017/9781108847148>.
- Swanner, E.D., Lambrecht, N., Wittkop, C., Harding, C., Katsev, S., Torgeson, J., and Poulton, S.W., 2020, The biogeochemistry of ferruginous lakes and past ferruginous oceans: *Earth-Science Reviews*, v. 211, <https://doi.org/10.1016/j.earscirev.2020.103430>.
- Swanner, E.D., Islam, R., Ledesma, G., Wittkop, C., Akam, S., Eitel, E., Katsev, S., Johnson, B., Poulton, S., and Bray, A., 2022, Geochemical Data from Sediments and Porewaters from Ferruginous and Meromictic Brownie Lake, Minnesota, U.S.A., Ver. 1: Environmental Data Initiative, <https://doi.org/10.6073/pasta/68b50baa0a767ab33f2b7dd91948036e> (accessed 7 September 2023).
- Thompson, K.J., Kenward, P.A., Bauer, K.W., Warchola, T., Gauger, T., Martinez, R., Simister, R.L., Michiels, C.C., Llíros, M., Reinhard, C.T., Kappler, A., Konhauser, K.O., and Crowe, S.A., 2019, Photoferrotrophy, deposition of banded iron formations, and methane production in Archean oceans: *Science Advances*, v. 5, <https://doi.org/10.1126/sciadv.aav2869>.
- Ward, L.M., Rasmussen, B., and Fischer, W.W., 2019, Primary productivity was limited by electron donors prior to the advent of oxygenic photosynthesis: *Journal of Geophysical Research: Biogeosciences*, v. 124, p. 211–226, <https://doi.org/10.1029/2018JG004679>.
- Wordsworth, R., and Pierrehumbert, R., 2013, Hydrogen-nitrogen greenhouse warming in Earth's early atmosphere: *Science*, v. 339, p. 64–67, <https://doi.org/10.1126/science.1225759>.
- Zahnle, K., Claire, M., and Catling, D., 2006, The loss of mass-independent fractionation in sulfur due to a Palaeoproterozoic collapse of atmospheric methane: *Geobiology*, v. 4, p. 271–283, <https://doi.org/10.1111/j.1472-4669.2006.00085.x>.

Printed in the USA